

# Intracellular Mechanics of Migrating Fibroblasts<sup>□</sup>

Thomas P. Kole, Yiider Tseng, Ingjye Jiang, Joseph L. Katz, and Denis Wirtz\*

Department of Chemical and Biomolecular Engineering, Johns Hopkins University, Baltimore, MD 21218

Submitted June 14, 2004; Revised September 28, 2004; Accepted October 1, 2004  
Monitoring Editor: Jennifer Lippincott-Schwartz

Cell migration is a highly coordinated process that occurs through the translation of biochemical signals into specific biomechanical events. The biochemical and structural properties of the proteins involved in cell motility, as well as their subcellular localization, have been studied extensively. However, how these proteins work in concert to generate the mechanical properties required to produce global motility is not well understood. Using intracellular microrheology and a fibroblast scratch-wound assay, we show that cytoskeleton reorganization produced by motility results in mechanical stiffening of both the leading lamella and the perinuclear region of motile cells. This effect is significantly more pronounced in the leading edge, suggesting that the mechanical properties of migrating fibroblasts are spatially coordinated. Disruption of the microtubule network by nocodazole treatment results in the arrest of cell migration and a loss of subcellular mechanical polarization; however, the overall mechanical properties of the cell remain mostly unchanged. Furthermore, we find that activation of Rac and Cdc42 in quiescent fibroblasts elicits mechanical behavior similar to that of migrating cells. We conclude that a polarized mechanics of the cytoskeleton is essential for directed cell migration and is coordinated through microtubules.

## INTRODUCTION

Cell migration is a cellular process that plays a critical role in health and disease, including embryogenesis, wound healing, immune response, and tissue development (Lauffenburger and Horwitz, 1996; Mitchison and Cramer, 1996; Pollard and Borisy, 2003). It is a highly regulated and coordinated process, which occurs through a myriad of signaling and structural proteins that orchestrate spatiotemporal reorganization of the actin cytoskeleton. Abnormal and/or unregulated cell motile behavior is known to contribute to several potentially fatal illnesses, including vascular disease and cancer (Ridley *et al.*, 2003).

Cell migration can be modeled as a repetitive, multistep process that begins with the establishment of spatial polarity and extension of membrane protrusions in the direction of movement. Newly formed protrusions are subsequently stabilized through firm adhesions to the underlying substrate and initiate contractile mechanisms that generate net forward motion and retraction of the trailing edge (Lauffenburger and Horwitz, 1996; Mitchison and Cramer, 1996; Pollard and Borisy, 2003). Every step of this cycle critically depends on the timely assembly, disassembly, and reorganization of actin filament structures that are mediated by members of the Rho family of small GTPases (Nobes and Hall, 1999). Overexpression of dominant negative variants of Rac and Cdc42 in fibroblasts reveals that Rac is necessary for membrane protrusion and the formation of wide lamella, whereas Cdc42 is required for the maintenance of cell polarity (Nobes and Hall, 1999).

Research over the past three decades has identified a myriad of structural and signaling proteins that regulate cell motility. However, how these proteins work in concert to modulate the physical properties of cytoskeleton networks and to generate net motion is uncertain. Brownian ratchet and elastic Brownian ratchet models (Peskin *et al.*, 1993; Mogilner and Oster, 1996) suggest that thermal fluctuations of the plasma membrane at the front of the cell are coupled to nucleated actin filament assembly to generate protrusive forces. Instead, motor-based models suggest that a barbed end directed motor protein such as myosin may push the membrane forward (Sheetz *et al.*, 1992). In these models of cell motility, the generation of net propulsive forces requires that the actin network at the leading edge is sufficiently stiff to avoid unproductive backward motion of the polymerizing filaments pushing against the plasma membrane, resulting in immediate force dissipation (Stossel, 1993; Lauffenburger and Horwitz, 1996; Mitchison and Cramer, 1996; Pollard and Borisy, 2003). It has been suggested that coordinated rearrangements of the cortical actin network can be accounted for by the dynamic behavior of F-actin cross-linking proteins, a model supported by *in vitro* studies by using reconstituted actin filament networks (Sato *et al.*, 1987; Wachsstock *et al.*, 1994), but untested in living cells. It is also unclear whether the cytoplasmic filament network stiffens or softens for cells to move. Indeed, diametrically opposed arguments can be made. One could speculate that for cell shape changes to occur in motile cells, the cytoskeleton has to be sufficiently soft. Vice versa, motile cells express much higher density of polymerized actin (Cramer *et al.*, 2002), which would increase the cytoskeleton network stiffness according to classical polymer physics.

The absence of a noninvasive method that probes local intracellular viscosity and elasticity has prevented a direct test of these hypotheses in living cells (Heidemann and Wirtz, 2004). Here, we use the recently developed method of intracellular microrheology (ICM) (Tseng *et al.*, 2002b) to explore the local intracellular mechanics of migrating fibroblasts. Intracellular mechanics measurements obtained in

Article published online ahead of print. Mol. Biol. Cell 10.1091/mbc.E04-06-0485. Article and publication date are available at [www.molbiolcell.org/cgi/doi/10.1091/mbc.E04-06-0485](http://www.molbiolcell.org/cgi/doi/10.1091/mbc.E04-06-0485).

<sup>□</sup> The online version of this article contains supplemental material at MBC Online (<http://www.molbiolcell.org>).

\* Corresponding author. E-mail address: [wirtz@jhu.edu](mailto:wirtz@jhu.edu).

this study demonstrate that both the lamella and perinuclear region of polarized cells are significantly stiffer than in quiescent cells. These results provide direct experimental evidence that cells adopt different mechanical properties to move. Our results also suggest that polarized migration of Swiss 3T3 fibroblasts results in a profound spatial polarization of the mechanical properties of the cytoskeleton, which is coordinated through microtubules. Further experiments exploring the intracellular mechanics of growth factor-stimulated activation of Rac and Cdc42 in quiescent Swiss 3T3 fibroblasts suggest that the mechanical role of these proteins is significantly magnified during cell migration.

## MATERIALS AND METHODS

### Cell Culture

Swiss 3T3 fibroblasts (American Type Culture Collection, Manassas, VA) were cultured in complete DMEM (c-DMEM; supplemented with 10% bovine calf serum; American Type Culture Collection) and maintained at 37°C in a humidified, 5% CO<sub>2</sub> environment. All multiple particle tracking microbiology (MPTM) measurements were performed in an incubator mounted on an inverted microscope maintained at 37°C with 5% CO<sub>2</sub> and humidity. Cells were grown on 35-mm glass-bottom dishes coated with poly-D-lysine (Mat-Tek., Ashland, MA) and treated with 50 μg/ml fibronectin (Calbiochem, San Diego, CA) for 1 h before plating.

### Reagents

Nocodazole (Sigma-Aldrich, St. Louis, MO) was prepared as a stock solution of 1 mg/ml in distilled water (dH<sub>2</sub>O). Platelet-derived growth factor (PDGF-BB) (Sigma-Aldrich) was prepared as a stock solution of 10 μg/ml in 4 mM HCl and 0.1% bovine serum albumin (wt/vol). Bradykinin (Sigma-Aldrich) was prepared as a stock solution of 25 mg/ml in dH<sub>2</sub>O.

### Scratch-Wound Experiments

Polarized migration of 3T3 fibroblasts was obtained using the scratch-wound model as described previously (DeBiasio *et al.*, 1987). Approximately  $1.0 \times 10^4$  cells were seeded into 35-mm glass-bottom dishes coated with poly-D-lysine (MatTek) and pretreated with 50 μg/ml fibronectin. Confluent monolayers were obtained after 3 d and wounded 1 d later by scraping through the middle of the dish by using a modified syringe needle. This method produced wounds that were consistently between 135 and 150 μm in width and closed within 6–6.5 h. After wounding, monolayers were immediately washed with c-DMEM and returned to the incubator for a 15-min recovery period. Monolayers used for intracellular mechanics experiments (Tseng *et al.*, 2002b) were microinjected along the wound edge with a solution of 0.1-μm red fluorescent carboxylate modified polystyrene microspheres (Molecular Probes, Eugene, OR) in Dulbecco's phosphate-buffered saline and then returned to the incubator. Wounded monolayers containing fluorescent microspheres were used in one of the following migration experiments: 1) control: wounded monolayers were removed from the incubator 4 h after initial wounding, and cells containing microspheres were used in our intracellular microrheology assay (see below, Intracellular Mechanics from Multiple Particle Tracking); 2) nocodazole: wounded monolayers were treated with c-DMEM supplemented with 1 μg/ml nocodazole 2 h after initial wounding and then returned to the incubator. Four hours after initial wounding, monolayers were removed from the incubator and cells containing microspheres were used in our intracellular microrheology assay.

### Intracellular Mechanics from Multiple Particle Tracking

To measure the local mechanical properties of cytoplasm, we used the method of intracellular microrheology introduced by Tseng *et al.* (Tseng *et al.*, 2002b; Kole *et al.*, 2004b). ICM consists of introducing fluorescent microspheres (0.1 μm) into the cytoplasm of living cell by using microinjection and then statistically analyzing their thermally excited motion to extract the local mechanical properties of the cytoskeletal network surrounding the particle. Particles embedded in the cytoplasm of living cells are equivalent to nanoscale rheometers that impose a locally time-averaged stress on the order  $k_B T/a^3$  of where  $k_B$  is the Boltzmann constant,  $T$  is the absolute temperature, and  $a$  is the particle radius. The resulting deformation is measured as the particle displacement and can be directly related to the local viscoelastic properties of cytoplasm.

Microinjected cells containing fluorescent particles were placed on the stage of a microscope at 37°C. Movies of the fluctuating fluorescent microspheres were recorded onto the random-access memory of a PC computer via a silicon-intensifier target camera (VE-100; Dage-MTI, Michigan City, IN) mounted on an inverted epifluorescence microscope (Eclipse TE300; Nikon, Melville, NY). A 100× Plan Fluor oil-immersion objective (numerical aperture

[NA] 1.3) was used for particle tracking, which permitted ~5-nm spatial resolution over a 120 × 120-μm field of view.

Movies of fluctuating microspheres were analyzed by a custom particle tracking routine incorporated into the MetaMorph imaging suite (Universal Imaging, West Chester, PA) as described previously (Tseng and Wirtz, 2001). The displacements of the particles centroids were simultaneously monitored in the focal plane of the microscope for 20 s at a rate of 30 frames/s. Three to five cells were tracked for each experimental condition yielding a total of ~100–200 microspheres per condition. Individual time-averaged mean-squared displacements (MSDs),

$$\langle \Delta r^2(\tau) \rangle = \langle [x(t + \tau) - x(t)]^2 + [y(t + \tau) - y(t)]^2 \rangle, \quad (1)$$

where  $\tau$  is the time scale and  $t$  the elapsed time, were calculated from the two-dimensional trajectories of the centroids of the microspheres. All control experiments are described in Tseng *et al.* (2002b), including effects of particle size and surface chemistry. It is important to note that the time scale of ICM experiments is much shorter than that of Swiss 3T3 fibroblast migration; therefore, cells are assumed to be stationary during the time of measurement. This is not the case for other particle tracking methods where the correlated motion between two particles is used instead of the motion of individual particles (Crocker *et al.*, 2000). These methods are inappropriate for the measurement of the mechanical properties of live cells because they incorrectly assume that the intracellular milieu is homogeneous and static. Furthermore, to obtain statistically significant data, measurement times are on the order of 30–60 min, time scales for which migrating cells cannot be assumed to be stationary.

MSDs of probe microspheres obtained from ICM experiments can be related to the shear creep compliance,  $\Gamma(\tau)$ , from the following relationship (Xu *et al.*, 1998):

$$\Gamma(\tau) = \frac{3k_B T}{2\pi a} \langle \Delta r^2(\tau) \rangle \quad (2)$$

The factor 3/2 stems from the fact we track the two-dimensional projection of the three-dimensional displacements of the probe microspheres. The creep compliance is a measure of the local deformability of the network surrounding the probe particle. It shares all of the same features as the MSD so that a perfectly viscous fluid will display a time scale-dependent creep compliance with a power law slope of 1, whereas a perfectly elastic solid will show a power law slope of 0 and a viscoelastic material, such as the cytoskeleton, will have a power law slope that lies between 0 and 1.

Local viscoelastic moduli of the intracellular milieu are calculated from MSDs by using a frequency-dependent form of the generalized Stokes-Einstein relationship (Mason *et al.*, 1997)

$$G^*(\omega) = \frac{k_B T}{\pi a i \omega \mathfrak{S}_r \{ \langle \Delta r^2(\tau) \rangle \}}, \quad (3)$$

where  $G^*(\omega)$  is the complex shear modulus,  $\omega$  is the deformation frequency, and

$$\mathfrak{S}_r \{ \langle \Delta r^2(\tau) \rangle \} \quad (4)$$

is the unilateral Fourier transform of the time-dependent MSD. The frequency-dependent elastic modulus  $G'(\omega)$  and loss modulus  $G''(\omega)$  are the real and imaginary parts, respectively, of the complex modulus and obey Kramers-Kronig relationships (Mason *et al.*, 1997; Dasgupta *et al.*, 2002). Bulk rheological measurements on standard and complex fluids made using a classical rheometer compare quantitatively (error <20%) with those obtained from our particle-tracking approach (Mason *et al.*, 1997).

Additionally, the translational diffusion coefficient,  $D$ , of a microsphere of radius  $a$  can be calculated from the Stokes-Einstein relationship (Einstein, 1905; Chandrasekhar, 1943; Qian *et al.*, 1991; Berg, 1993):

$$D = \frac{k_B T}{6\pi a \eta}, \quad (5)$$

where  $\eta$  is the shear viscosity of the fluid surrounding the particle and can be approximated as the product of the relaxation time (the time scale at which the viscous-to-elastic crossover occurs; Figure 1) and the plateau value of the elastic modulus (Eckstein *et al.*, 1998). The diffusion coefficient calculated from two-dimensional particle trajectories can be approximated as the three-dimensional diffusion coefficient assuming that the local environment surrounding each microsphere is isotropic in three dimensions. This is a valid approximation, even in regions of the cell where long-range interactions between microspheres and the cell membrane could occur via hydrodynamic interactions, because those interactions are screened to within a mesh size of the surrounding network, which is ~50 nm. If the cell thickness were similar or smaller than the particle diameter, they would be mostly excluded from those (too thin) areas. In our experiments, injected particles were rarely, if ever, located at the edge of the lamellipodium where thin membrane ruffling and retrograde actin flow occur.

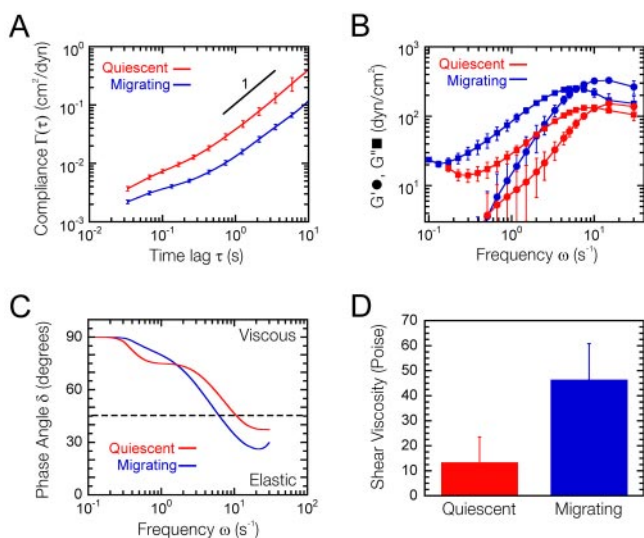


**Figure 1.** Intracellular mechanical properties of migrating cells. (A) Mean cellular deformability directly computed from the mean-squared displacements of the thermal motions of microspheres injected into the cytoplasm of serum-starved Swiss 3T3 cells (red) and Swiss 3T3 cells at the edge of a wounded monolayer (blue) 4 h after wounding ( $n = 5$  cells). Error bars denote SE of measurement. (B) Frequency-dependent viscous and elastic moduli of cytoplasm,  $G'(\omega)$  (circles) and  $G''(\omega)$  (squares), calculated from mean cellular deformability (A). (C) Frequency-dependent phase angle,  $\delta = \tan^{-1}(G''/G')$ , calculated from viscoelastic moduli (B). (D) Shear viscosity of cytoplasm obtained from the product of the plateau modulus and relaxation time (B).

### Fluorescence Microscopy

After each microrheology experiment was completed, cells were immediately fixed and immunostained to quantify the orientation of the microtubule organizing center (MTOC). Cells were fixed in 2.5% paraformaldehyde in phosphate-buffered saline (Invitrogen, Carlsbad, CA), and permeabilized in 0.1% Triton X-100 (Sigma-Aldrich) in phosphate-buffered saline. Cells were blocked in 10% fetal bovine serum for 30 min at room temperature and labeled with an  $\alpha$ -tubulin monoclonal antibody (mAb) at 1:100 (Oncogene Research, Cambridge, MA) dilution for 1 h. Monolayers were subsequently labeled with Alexa 488 anti-mouse at 1:50 (Molecular Probes). Coverslips were mounted in Antifade (Molecular Probes) to minimize photobleaching. Fluorescently labeled cells were observed with a 60 $\times$  oil-immersion objective (NA 1.4) mounted on a Nikon Eclipse TE300 inverted microscope. Images were acquired with an Orca II charge-coupled device (CCD) camera (Hamamatsu, Bridgewater, NJ) controlled by the MetaMorph software.

Experiments also were performed to quantify the organization of the actin cytoskeleton and distribution of vinculin-containing adhesions in cells at the edges of wounded fibroblast monolayers. Wounded monolayers were fixed each hour for 6 h after wounding, starting at  $t = 0$  h. Monolayers were permeabilized, blocked, and labeled with a vinculin mAb (Sigma-Aldrich) at 1:100 dilution for 1 h. Monolayers were subsequently labeled with Alexa 488 phalloidin at 1:40 (Molecular Probes) and Alexa 540 anti-mouse at 1:50 (Molecular Probes) and imaged as described above.

### Phase Contrast Microscopy

The subcellular organization and morphology of live cells were revealed using phase contrast microscopy via a 60 $\times$  oil-immersion Plan Fluor lens (NA 1.4) (Nikon). This lens was mounted on a Nikon Eclipse TE300 inverted microscope. Images were acquired with an Orca II CCD camera controlled by the MetaMorph software.

## RESULTS

### Mean Intracellular Mechanics of Migrating and Nonmigrating Fibroblasts

To investigate the intracellular mechanics of cell migration, we adopted the wounded fibroblast monolayer system as described by DeBiasio *et al.* (1987) and combined it with

intracellular microrheology recently introduced by Tseng *et al.* (2002a,b) and Kole *et al.*, 2004a,b. A confluent monolayer of Swiss 3T3 fibroblasts was scraped to produce a wound of  $\sim 140$   $\mu\text{m}$  in width (Supplementary Figure 1), and cells along the wound edge were subsequently microinjected with 0.1- $\mu\text{m}$  red-fluorescent microspheres. Within 1 h, cells along the wound edge developed a polarized morphology with membrane protrusions (lamellipodia and filopodia) that extended into the wound, whereas cells maintained close lateral contact with their neighbors. After  $\sim 6$  h, cells at the two edges began to meet and lost their polarized morphology. To facilitate the distribution of injected microspheres throughout the cell, we chose to conduct all of our intracellular mechanics experiments 4 h after wounding. At 4 h, wounds were  $\sim 70\%$  closed, and wounded edge fibroblasts possessed a polarized morphology characterized by the positioning of the MTOC toward the wound as well as a wide extended lamella (Supplementary Figure 1).

The local mechanical properties of the migrating fibroblasts were calculated from the nanometer-scale displacements,  $[x(t), y(t)]$ , where  $t$  is the elapsed time of injected microspheres as measured by video-based particle nano-tracking. Particle trajectories were transformed into time-averaged MSDs, creep compliance (i.e., deformability) profiles (Figure 1A), and frequency-dependent viscoelastic moduli (Figure 1B). Details about the method of ICM can be found in Tseng *et al.* (2002b) and Kole *et al.*, 2004a,b, which offers a thorough description of control experiments involving microspheres of different size and surface chemistry. Importantly, during the short time of movie capture (20 s), the displacements of the cell were much smaller than the displacements of the microspheres. Therefore, our particle tracking measurements are unaffected by the bulk movement of the cell.

Examination of the mean cellular deformability of both migrating and quiescent 3T3 fibroblasts reveals that the overall mechanical properties of the cell changed dramatically upon migration (Figure 1A). Cells along the edge of a wounded fibroblast monolayer were significantly less deformable (i.e., stiffer) than quiescent fibroblasts, as shown by the approximately threefold decrease in the mean cellular deformability. To test the statistical significance of this difference, we can use the  $p$  value obtained from a two-tailed  $t$  test with a 95% confidence level. However, due to the time-scale dependence of the cellular deformability, we instead performed  $t$  tests at each time scale from 0.033 to 10 s and then averaged the calculated  $p$  values to obtain an average  $p$  value. The average  $p$  value was  $\ll 0.05$ ; therefore, the difference in the deformability profiles of quiescent and migrating cells was statistically significant.

Transformation of MSDs into frequency-dependent viscoelastic moduli (see *Materials and Methods*) shows that the cytoskeleton of migrating and quiescent cells exhibited significantly different types of mechanical behavior. The local elastic and viscous moduli  $G'(\omega)$  and  $G''(\omega)$  (Figure 1B) of the cytoplasm were directly calculated from MSD as described previously (Mason *et al.*, 1997; Dasgupta *et al.*, 2002). The moduli  $G'(\omega)$  and  $G''(\omega)$ , respectively, characterize the elasticity (i.e., the propensity of the cytoplasm to rebound after a force is applied) and the dynamic viscosity of cytoplasm as a function of deformation frequency,  $\omega$ , which is simply the inverse of the time scale used in MSD calculations. We note that the units of compliance ( $\text{cm}^2/\text{dyn}$ ) (Figure 1A) are the inverse of the units of  $G'(\omega)$  and  $G''(\omega)$  ( $\text{dyn}/\text{cm}^2$ ) (Figure 1B), i.e., a more elastic/viscous material is less susceptible to deformation. The plateau value of the elastic modulus of wounded edge fibroblasts was almost 3 times that of quies-

cent fibroblasts (Figure 1B), which means that cell migration coincides with a dramatic increase in the elasticity of the cytoskeleton. This effect was not limited to elasticity; cell motility also had a pronounced effect upon intracellular viscosity. The relative contributions of viscosity and elasticity to the overall viscoelastic response of the cytoplasm was evaluated by the phase angle,  $\delta = \tan^{-1}(G''/G')$  (Figure 1C), which reveals whether a material behaves like a Hookean solid ( $\delta = 0^\circ$ ); a viscous liquid ( $\delta = 90^\circ$ ); or a viscoelastic element ( $0^\circ < \delta < 90^\circ$ ) (Coulombe *et al.*, 2000). Both quiescent and migrating fibroblasts exhibited phase angle profiles that were nearly  $90^\circ$  at low frequencies and rapidly decreased with increasing frequency. Over the measured frequency range (0.1–30 Hz), migrating fibroblasts exhibited a biphasic mechanical behavior, where the cell displayed viscoelastic-liquid behavior ( $\delta > 45^\circ$ ) at low frequencies ( $\tau > 0.2$  s) and a viscoelastic solid behavior ( $\delta < 45^\circ$ ) at high frequencies ( $\tau < 0.2$  s). The crossover frequency at which  $\delta = 45^\circ$  corresponds to the inverse of the relaxation time ( $\tau = 0.2$  s) at which the local network, subjected to the fluctuating particle, begins to flow. This means that when (locally) sheared rapidly, the cytoplasm of a migrating cell behaved mostly like a stiff solid, whereas when sheared slowly the cytoplasm behaved mostly like a viscous liquid. Quiescent cells followed a similar trend, albeit the range of frequencies over which elasticity dominated viscosity was narrower ( $\tau < 0.09$  s). The more solid-like behavior of migrating cells makes them more able to elastically rebound under mechanical stress and therefore potentially less prone to mechanical failure that may be important *in vivo* where cells are migrating through dense connective tissues and/or on the endothelium against venous/arterial shear flow.

Cell migration has been associated with increased transport of intracellular vesicles using cytoskeletal motor protein assemblies (Gundersen, 2002; Rodriguez *et al.*, 2003), putatively to supply the leading edge with components to form new protrusions and adhesions. Vesicle trafficking through the cytoplasm has to overcome the viscous frictional resistance of the cytoskeleton. From our mechanical measurements, we obtain values for the shear viscosity of the cytoskeleton (Figure 1D) from the product of the relaxation time (inverse of the frequency where  $G' = G''$ ,  $\delta = 45^\circ$ ) and the plateau modulus (the value of the elastic modulus evaluated at the frequency where the minimum of  $\delta$  occurs, *i.e.*, maximum elasticity) (Eckstein *et al.*, 1998). Our results show that, in migrating cells, the intracellular shear viscosity increased from  $13.4 \pm 10.1$  Poise to  $46.5 \pm 14.4$  Poise, suggesting that the transport of 0.1- $\mu\text{m}$  particles within the cytoplasm of migrating cells is almost 4 times more difficult than in quiescent cells. The difference in viscosity between quiescent and motile cells is similar to the difference between the viscosity of corn syrup ( $\sim 25$  Poise) and the viscosity of honey ( $\sim 80$  Poise) at  $20^\circ\text{C}$ .

### Local Mechanics of Migrating Fibroblasts

To examine the local intracellular mechanics of migrating cells, we color-coded subcellular regions corresponding to the location of injected tracer particles according to the local value of the cellular deformability at a time scale of 1 s, obtained from intracellular microrheology measurements (Figure 2). We only show tracked particles and we increase their size to facilitate visualization; therefore, particles depicted in Figure 2 do not reflect their actual size (0.1  $\mu\text{m}$ ). The cell shown in Figure 2 displays a polarized morphology with its nucleus positioned toward the rear of the cell, and leading edge extending into the wound in the direction of migration. From the local color coding scale where blue

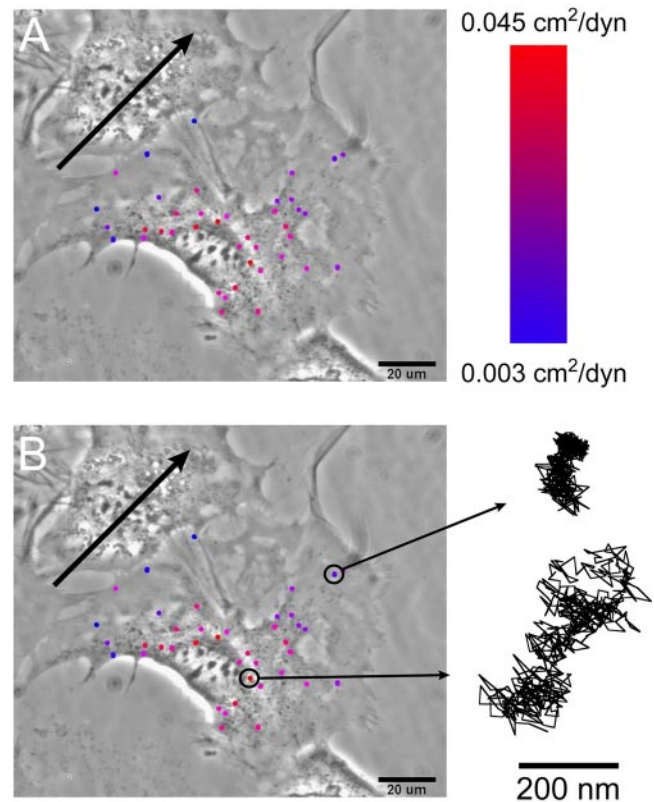


**Figure 2.** Local mechanics of cell migration. (A and B) Phase contrast micrographs of a Swiss 3T3 fibroblast at the edge of a wounded monolayer 4 h after wounding overlaid with fluorescent micrographs of fluorescent microspheres injected into the cytoplasm. Here, we only show tracked single particles and neglected (the few) particle aggregates, which have an unknown size and therefore make evaluation of the local moduli difficult. Each particle position was color-coded corresponding to the local value of the deformability at a time scale of 1 s. Note that the color indicators at each particle position do not reflect the size of the particle (0.1  $\mu\text{m}$ ). Indicator size was increased to aid visual presentation. Blue denotes the least deformable (stiffest) regions of the cell; red denotes the most deformable (softest) regions. Arrow denotes the direction of the wound. (B) Typical trajectories of microspheres embedded in regions near the leading edge and perinuclear region of a migrating fibroblast. Scale bar indicates length scale for both trajectories.

corresponds to the regions of lowest compliance (least deformable or stiffest) and red to the regions of highest compliance (most deformable or softest), it is apparent that the leading edge of the cell and peripheral regions furthest from the nucleus are stiffer than perinuclear regions (Figure 2A). This is illustrated by the trajectories of particles closest to the wound edge and those closest to the nucleus (Figure 2B). Particles at the cell periphery display significantly smaller displacements because their cytoskeleton microenvironment is stiffer than particles embedded regions near the nucleus. We note that the trajectories shown in Figure 2B are asymmetric. This is not because of bulk motion of the cell, which is negligible during data collection (20 s), but because the trajectories of Brownian particles are always anisotropic (*i.e.*, not symmetric) even in the absence of bulk flow (Haber *et al.*, 2000).

We can quantitatively compare the micromechanical differences between the perinuclear and lamella regions of migrating cells by defining the perinuclear region as the

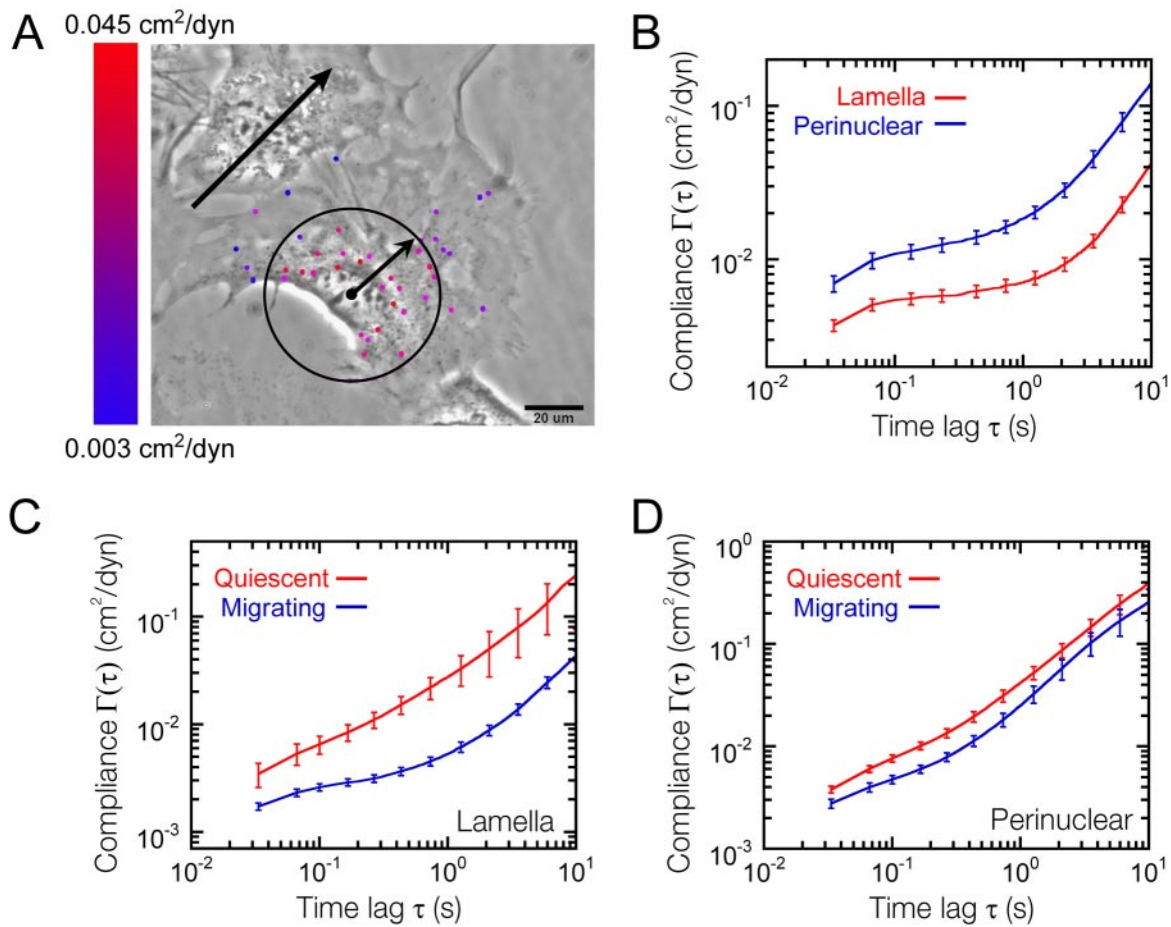


**Figure 3.** Spatial polarization of the mechanical properties of migrating cells. (A) Phase contrast micrograph of a Swiss 3T3 fibroblast at the edge of a wounded monolayer 4 h after wounding overlaid with a fluorescent micrograph of fluorescent microspheres injected into the cytoplasm. A 30- $\mu\text{m}$  radius was drawn from the center of the nucleus to define the perinuclear (inside) and lamella (outside) regions. Arrow denotes the direction of the wound. (B) Regionally averaged deformability of the perinuclear and lamella regions of the cell shown in A. (C) Comparison of the lamella-averaged deformability of quiescent (red,  $n = 5$  cells) and migrating fibroblasts (blue,  $n = 5$  cells). (D) Comparison of the perinuclear-averaged deformability of quiescent (red) and migrating fibroblasts (blue).

region encompassed by a circle of radius 30  $\mu\text{m}$  with origin at the center of the nucleus (Figure 3A) and the lamella as the remaining portion of the cell. We empirically chose this radius because, for all cells measured, it formed a circle that encompassed almost all of the subcellular organelles (as detected by phase contrast microscopy). For illustration, the region-averaged deformability of the cell shown in Figure 3B confirms that the lamella of wounded edge fibroblasts is significantly (average  $p$  value  $\ll 0.05$ ) less compliant (stiffer) than the perinuclear region. This behavior was not isolated to this particular cell but was observed for all measured cells ( $n = 5$ ; our unpublished data). It is important to note that the observed difference in the magnitude of the deformability of the perinuclear and lamella regions is dependent upon the chosen size of the perinuclear region (radius from center of nucleus); however, the trend is consistent for radii of  $30 \pm 5 \mu\text{m}$ . In contrast to the regionally correlated mechanical properties of migrating cells, the regionally averaged deformability of the lamella and perinuclear regions of quiescent cells are similar (Figure 3, C and D). The lamella of migrating cells was approximately 4 times stiffer than that of quiescent cells, whereas the perinuclear regions were similar (Figure 3). Together, these results suggest that cell migration

results in a spatially polarized distribution of the local mechanical properties of the cell.

#### Micromechanical Role of Microtubules in Cell Migration

Microtubules play a critical role in the maintenance of cell polarity during cell migration in many cell types, including fibroblasts (Vasiliev *et al.*, 1970; Goldman, 1971; Bershadsky *et al.*, 1991). Treatment of wounded 3T3 fibroblast monolayers with the microtubule depolymerizing agent nocodazole results in loss of cell polarity and inhibition of wound closure (Magdalena *et al.*, 2003). To investigate a possible mechanical role for microtubules in cell motility, we repeated our intracellular microrheology experiments, this time with wounded edge cells treated with 1  $\mu\text{g}/\text{ml}$  nocodazole in c-DMEM 2 h after scraping. Wounded edge fibroblasts treated with 1  $\mu\text{g}/\text{ml}$  nocodazole displayed very few intact microtubules and almost complete loss of motility (our unpublished data), whereas their overall morphology remained similar to untreated cells (Figure 5A). The disruption of microtubules had limited effect upon the overall mechanical properties of migrating fibroblasts (Figure 4). The mean deformability of control (untreated) wounded edge fibroblasts was nearly identical to that of nocodazole-

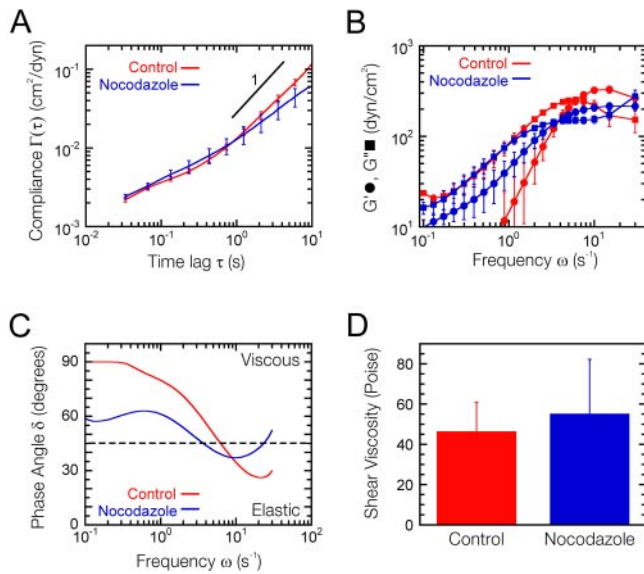


**Figure 4.** Loss of microtubules has little effect upon the overall mechanical properties of migrating cells. (A) Mean cellular deformability directly computed from the mean-squared displacements of the thermal motions of microspheres injected into the cytoplasm of Swiss 3T3 cells at the edge of a wounded monolayer (blue) treated with 1  $\mu$ g/ml nocodazole 2 h after wounding and compared with the mean deformability of untreated migrating cells (red) 4 h after wounding ( $n = 5$  cells). (B) Frequency-dependent viscous and elastic moduli of cytoplasm,  $G'(\omega)$  (circles) and  $G''(\omega)$  (squares), calculated from mean cellular deformability (A). (C) Frequency-dependent phase angle,  $\delta(\omega) = \tan^{-1} [G''(\omega)/G'(\omega)]$ , calculated from viscoelastic moduli (B). (D) Shear viscosity of cytoplasm obtained from the product of the plateau modulus and relaxation time (B).

treated cells. Similarly, the shear viscosity of control and nocodazole wounded cells was similar. Nevertheless, there was a slight decrease in the plateau value of the elastic modulus, from  $325 \pm 25$  to  $217 \pm 19$  dyn/cm<sup>2</sup>, and a shift in the frequency at which the viscous to elastic cross over occurred in nocodazole-treated cells, from 6.2 to 3.3 Hz (Figure 4C).

Inspection of the local mechanical properties of nocodazole-treated wounded fibroblast monolayers reveals a somewhat different behavior than in control cells. Both the lamella and perinuclear region of the cell shown in Figure 5A contain a mixture of red (soft) and blue (stiff) regions, which is reflected in the region-averaged cellular deformabilities (Figure 5B) that are statistically indistinguishable at the 95% confidence level. This trend was observed in most nocodazole-treated cells ( $n = 5$ ; our unpublished data). Comparison of the deformability of lamella and perinuclear regions averaged over all nocodazole-treated cells with those of untreated migrating fibroblasts (Figure 5, C and D) shows that microtubule depolymerization has a much greater effect upon the mechanical properties of the lamella region than the perinuclear region of the cell. These results suggest that microtubules play a key role in the polarization of the mechanical properties of migrating cells.

#### RhoGTPases and the Micromechanics of Cell Migration

Members of the Rho family of small GTPases have been well established as key regulators of cell motility (Nobes and Hall, 1999; Ridley *et al.*, 2003). Polarized migration of many cell types have been shown to be critically dependent upon

localized activation of Rac, which is mediated by Cdc42 (Nobes and Hall, 1999; Kraynov *et al.*, 2000). To test whether Rac or Cdc42 could be responsible for the increased overall elasticity and viscosity observed in migrating cells compared with quiescent cells (Figure 1), quiescent Swiss 3T3 fibroblasts were treated with the Cdc42 agonist bradykinin or the potent Rac activator PDGF. Bradykinin has been shown to promote the formation of Cdc42-dependent membrane protrusions in serum-starved fibroblasts (Figure 6A) (Kozma *et al.*, 1995), whereas PDGF stimulates the Rac-dependent formation of membrane ruffles and lamellipodia (Figure 6B) (Ridley *et al.*, 1992). Treatment of serum-starved Swiss 3T3 fibroblasts with 100 ng/ml bradykinin had little effect upon the deformability of the cell (Figure 6C) and only modest changes in the plateau modulus and shear viscosity (Figure 6D). PDGF (10 ng/ml) had a greater effect than bradykinin (Figure 6, C and D). However, mechanical response was significantly attenuated in comparison to that observed in migrating cells.

To examine the regional mechanics of cells after Rac and Cdc42 activation, cells were color-coded according to the local value of the cellular deformability before and after 10-min treatment with PDGF or bradykinin (Figure 7A). The lamella region of PDGF-treated cells was significantly stiffer than untreated cells (Figure 7B), whereas bradykinin had little effect. PDGF treatment also resulted in a reduction of the deformability (i.e., stiffening) of the perinuclear region; however, bradykinin had no significant effect upon the mechanical properties (Figure 7C). Together, these results suggest that Rac is at least partly responsible for the mechanical stiffening of migrating fibroblasts. Scratch-wound ICM experiments by using fibroblasts injected with fluorescent microspheres and green fluorescent protein (GFP) plasmids encoding Cdc42-T17N (dominant negative) 4 h before measurement suggest that Cdc42 may affect the differential distribution of the local mechanical properties of migrating cells (our unpublished data). However, GFP-Cdc42-T17N expression greatly varied between cells, as determined by GFP intensity, which was probably due to the short (4-h) incubation time.

## DISCUSSION

### Regional Mechanics of Cytoskeleton during Cell Migration

It has long been speculated that cytoskeleton rearrangements elicit local changes in the physical properties of the cytoskeleton, specifically its local elasticity and viscosity, to facilitate cell migration (Sato *et al.*, 1987; Stossel, 1993). However, the absence of noninvasive methods that probe local intracellular viscoelastic parameters have prevented a direct test of that hypothesis (Heidemann and Wirtz, 2004). Intracellular mechanics measurements presented in this study demonstrate that both the periphery and perinuclear region are significantly stiffer in polarized cells than in quiescent cells. These results provide direct experimental evidence that cells adopt dramatically different mechanical properties to move. Increased stiffness of the cell cortex may help motile cells produce net actin-powered propulsive forces by preventing unproductive rearward movements of the filaments pushing against the plasma membrane (Borisy and Svitkina, 2000). Our results disagree with those obtained in a prior study examining the mechanical properties of migrating fibroblasts by using scanning probe microscopy (Nagayama *et al.*, 2001), where it was suggested that the mechanical properties of the cytoskeleton actually soften upon

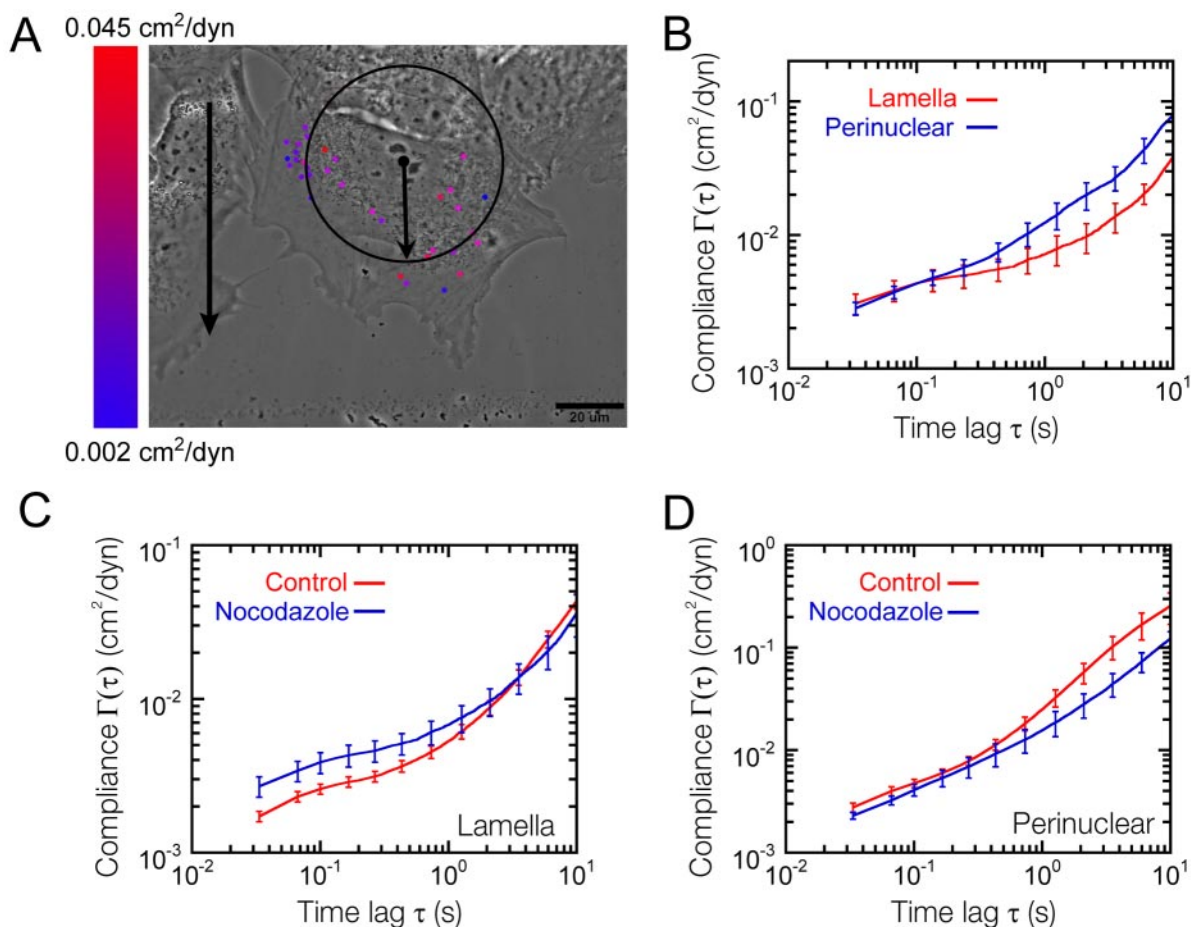


**Figure 5.** Microtubule depolymerization effects the local mechanical properties of migrating cells. (A) Phase contrast micrograph of a Swiss 3T3 fibroblast at the edge of a wounded monolayer treated with 1  $\mu\text{g}/\text{ml}$  nocodazole 2 h after wounding overlaid with a fluorescent micrograph of fluorescent microspheres injected into the cytoplasm. A 30- $\mu\text{m}$  radius was drawn from the center of the nucleus to define the perinuclear (inside) and lamella (outside) regions. Arrow denotes the direction of the wound. (B) Regionally averaged deformability of the perinuclear and lamella regions of the cell shown in A. (C) Comparison of the lamella-averaged deformability of untreated migrating fibroblasts (red,  $n = 5$  cells) with 1  $\mu\text{g}/\text{ml}$  nocodazole-treated migrating fibroblasts (blue,  $n = 5$  cells). (D) Comparison of the perinuclear-averaged deformability of untreated migrating fibroblasts (red) with 1  $\mu\text{g}/\text{ml}$  nocodazole-treated migrating fibroblasts (blue).

migration. However, the technique used in that study does not measure intracellular mechanical properties and should not be used to examine cytoskeleton dynamics (see more below).

Cell migration is controlled by the spatiotemporal activation/deactivation of Rho GTPases, which mediates local remodeling and contractility of cytoskeletal structures and the local mechanical properties of the cell (Kole *et al.*, 2004a) (Figure 8). However, the pronounced increase in the intracellular mechanical stiffness of migrating fibroblasts compared with quiescent fibroblasts (160%) cannot simply be accounted for by the activation of Rho, Rac, or Cdc42. Previously, we demonstrated that activation of Rho induces global mechanical stiffening of quiescent fibroblasts that resulted in a 94% increase in the plateau modulus (Kole *et al.*, 2004a). In the present study, we find that activation of Cdc42 through bradykinin treatment of quiescent Swiss 3T3 fibroblasts results in a minor reduction of the plateau modulus (20%), whereas activation of Rac through PDGF treatment only results in a relatively modest 50% increase of the plateau modulus. Activation of Rac does, however, result in stiffening of both the perinuclear and lamella regions of the cell (Figure 8). The observed trend is similar to that of

migrating cells where micromechanical stiffening is significantly more pronounced in the lamella region of the cell. These results indicate that cell migration may involve the activation of actin cross-linking proteins whose activity are not mediated by growth factor induced activation of Rho, Rac, or Cdc42.

#### *Cytoskeleton of Motile Cells Behaves as a Dynamically Cross-linked Polymer Network*

As mentioned previously, cell migration requires the cytoskeleton to be both sufficiently elastic to help growing filaments generate productive forces and sufficiently soft to allow cell shape changes. Our measurements show that the overall mechanical behavior of the cytoskeleton of motile cells is elastic at short time scales ( $\tau < 0.2$  s) and liquid-like at long time scales ( $\tau > 0.2$  s); however, the elastically dominated regime is extended in the lamella ( $\tau < 1$  s). Therefore, only fast cytoskeletal changes occurring on time scales  $< 1$  s have a significant elastic component. The enhanced elasticity of the cytoskeleton in motile cells help provide the pointed ends of the polymerizing filaments with a stiff support to push against before the membrane protrusions are stabilized by focal attachments to the substratum.

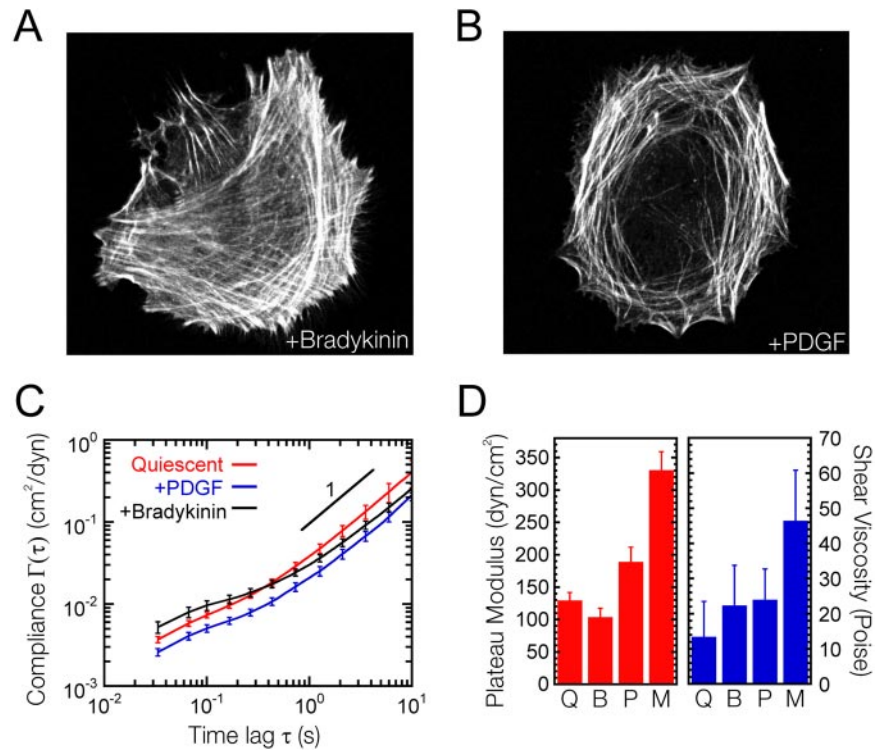


**Figure 6.** Mechanical effects of Cdc42 and Rac activation in serum-starved Swiss 3T3 fibroblasts. (A and B) Fluorescent micrographs of serum-starved Swiss 3T3 cells treated with 100 ng/ml bradykinin for 10 min (A), or 10 ng/ml PDGF for 10 min (B). Actin filaments (white) were visualized with Alexa 488 phalloidin. (C) Mean cellular deformability directly computed from the mean-squared displacements of the thermal motions of microspheres injected into the cytoplasm of serum-starved Swiss 3T3 cells before (red) and after treatment with 10 ng/ml PDGF for 10 min (blue), or 100 ng/ml bradykinin for 10 min (black). (D) Shear viscosity and plateau modulus of quiescent (Q), bradykinin (B)-treated, PDGF (P)-treated, and migrating (M) Swiss 3T3 fibroblasts.

It will be interesting to correlate directly the rate of protrusion formation in different types of cells with the crossover rate between elastic and viscous behavior.

Viscoelastic behavior of complex fluids is ubiquitous for both polymeric and protein systems; however, it has largely been ignored in live cells and often misinterpreted as tensegrity. According to the tensegrity model, cell shape and structure are determined by the balance of tensile loads generated by actin and intermediate filaments against compression-resistant microtubule struts, and therefore forces applied to local regions of the cytoskeleton are transferred throughout the cell (Maniotis *et al.*, 1997). In an attempt to validate this model, Maniotis *et al.* (1997) showed that applying large deformations to the actin cytoskeleton of permeabilized endothelial cells via arginine-glycine-aspartic acid-coated microspheres attached to integrin receptors on the surface resulted in reorientation of cytoskeletal filaments and distortion of the nucleus. The authors claim that this demonstrates the mechanical continuity of the cell and that the nucleus is “hard-wired” to the cytoskeleton. After examining the large rates of deformation that were applied to cells using their system (5–10  $\mu\text{m/s}$ ) and our own data from this and previous studies (Tseng *et al.*, 2002b; Kole *et al.*, 2004a,b), we argue that what they observed was actually an elastic response from the cytoskeleton in the high frequency regime and not tensegrity.

Viscoelastic transformations observed in live cells can be accounted for by the dynamic behavior of F-actin cross-linking proteins, as suggested by *in vitro* models of cytoskeleton mechanics (Sato *et al.*, 1987; Wachsstock *et al.*, 1994). Actin filament networks in the presence of the dynamic cross-linking protein  $\alpha$ -actinin stiffen under high-rate deformations and deform readily under slow deformation (Sato *et al.*, 1987). However, studies of the cross-linking protein filamin, which localizes to the periphery of motile cells (Flanagan *et al.*, 2001), suggest that cortical actin is rheologically equivalent to a covalently cross-linked gel (Janmey *et al.*,

1990), i.e., it behaves like a piece of rubber whose stiffness is independent of the rate of deformation and elastically dominated at all time scales. To deform, the cytoskeleton would rely on mechanisms that modulate network stiffness through the regulation of filament length or interfilament cross-linking. Our intracellular mechanics measurements in live cells, which probe local viscoelastic behavior as a function of the rate of deformation (frequency,  $\omega$ , in Figure 1B), allow us to distinguish one model from the other. Our measurements show that the cytoskeleton of both motile and quiescent cells deform relatively easily at low frequencies and deform little at high frequencies. This result strongly supports the notion that, from a rheological standpoint, actin-rich networks *in vivo* do not behave like permanently cross-linked networks. Recent careful biochemical studies confirm that the bimodal behavior of the cytoskeleton *in vivo* can be reproduced with reconstituted actin networks containing not only  $\alpha$ -actinin (Xu *et al.*, 2000) but also with filamin at relatively low concentrations (Tseng *et al.*, 2004). The frequency-dependent viscoelastic properties of the cytoskeleton are particularly well adapted to fast motility events such as membrane ruffling in motile cells.

Agreement between intracellular mechanics *in vivo* and mechanics of reconstituted cytoskeleton networks *in vitro* is quantitative. It has long been believed that elastic moduli of tissue culture cells are much higher than those measured in reconstituted actin filament networks *in vitro*. This assessment has been based on previous measurements of cell mechanics. However, previous cell mechanics measurements (using atomic force microscopy, calibrated micropipettes, magnetocytometry, or parallel plates) have inferred the viscoelastic properties of the cytoskeleton from extracellular measurements and have relied on the ill-defined contact with the cell plasma membrane and the probe. Extracellular methods measure moduli in the  $\sim 1000$  Pa range, hundreds of times those measured *in vitro* and measured here by intracellular microrheology. Hence, although valu-

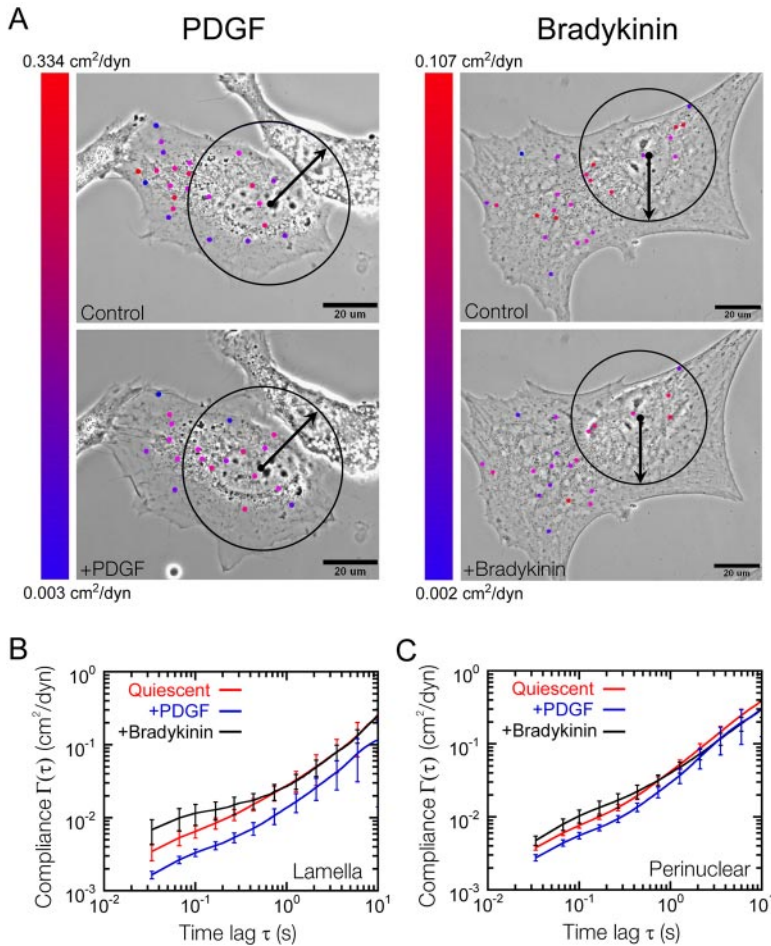


**Figure 7.** Local mechanics of Rac and Cdc42 activation. (A) Phase contrast micrographs of serum-starved Swiss 3T3 fibroblasts before and after treatment with 10 ng/ml PDGF for 10 min or 100 ng/ml bradykinin for 10 min. A 30- $\mu\text{m}$  radius was drawn from the center of the nucleus to define the perinuclear (inside) and lamella (outside) regions. (B) Comparison of the lamella-averaged deformability of serum-starved Swiss 3T3 cells before (red) and after treatment with 10 ng/ml PDGF for 10 min (blue) or 100 ng/ml bradykinin for 10 min (black). (C) Comparison of the perinuclear-averaged deformability of serum-starved Swiss 3T3 cells before (red) and after treatment with 10 ng/ml PDGF for 10 min (blue) or 100 ng/ml bradykinin for 10 min (black).

able to assess membrane and submembrane mechanics, these methods should not be used to assess bulk cytoskeleton mechanics. The quantitative agreement (amplitude of viscoelasticity, frequency dependence of these parameters) between *in vivo* measurements presented here and those obtained with reconstituted cytoskeleton networks has two important implications. 1) This agreement (further) justifies the use of reductionist models of cell motility and cell mechanics that make use of purified proteins (Pollard, 2003). 2) It suggests that the influential Brownian (elastic) ratchet model of cell motility requires adjustment (Mogilner and Oster, 1996, 2003). That model relies on viscoelastic moduli of the lamella in the  $\sim 1000$  Pa range to predict net forces from the polymerization of actin filaments in the lamellipodia. Actin filaments close to the edge of the cell must have a stiff foundation to push against to produce directed forces due to polymerization; however, we show that the stiffness of the lamella is on the order of 10s of Pascals, not 1000s of Pascals. Although we are unable to probe the very edge of the cell, we do not expect its stiffness to be significantly greater than that which we measured in the lamella, based upon the fact that the values measured from all regions of the cell only vary by approximately 2 orders of magnitude.

#### *Spatial Polarization of the Intracellular Mechanical Properties of Migrating Cells*

We have shown that migrating cells at the edge of a wounded fibroblast monolayer display spatial polarization of their intracellular mechanical properties where the stiffest

or most elastic regions of the cytoskeleton are located toward the edge of the cell in the direction of migration. It has been previously demonstrated that this subcellular region correlates with the highest ratio of F-actin/G-actin (Cramer *et al.*, 2002) and is consistent with our previous findings that actin polymerization and the formation of entangled networks provides a significant contribution to the intracellular mechanical properties of the cell (Kole *et al.*, 2004a). This may facilitate cell migration by providing mechanical stability to cellular protrusions that work against the elasticity of the plasma membrane and surrounding tissues.

However, elevated levels of mechanical stiffness toward the leading edge also may work against the cell. Intracellular cargo, including membrane components and associated proteins needed for the formation of new protrusions, is transported from the Golgi apparatus toward the leading edge along microtubule tracks by using ATP-driven motor protein assemblies (Gundersen, 2002; Rodriguez *et al.*, 2003). The force that must be generated by a protein motor to move a vesicle through the cell is dependent upon local frictional forces between the vesicle and intracellular milieu, which result from the local mechanical properties of the cytoskeleton (Holzwarth *et al.*, 2002). Using the shear viscosity measured by ICM, we can calculate the magnitude of the propulsive forces required to promote the directed motion of viral particles, endosomes, or gene carriers within the cytoplasm.

The minimal propulsive force required to generate directed motion is approximately given by the product of the

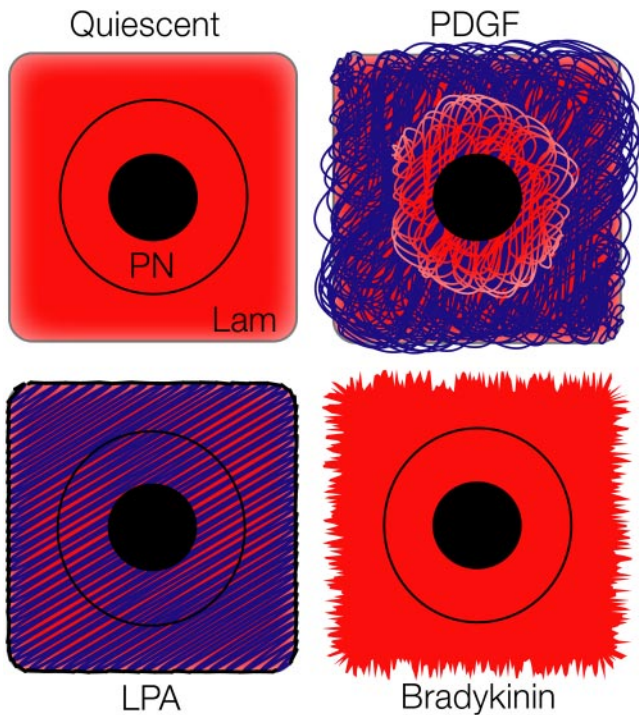


**Figure 8.** Summary of intracellular mechanics of growth factor stimulated Rho GTPase activation. Addition of extracellular growth factors induces local changes in the mechanical properties of quiescent Swiss 3T3 fibroblasts. Areas colored red denote the softest regions of the cell, whereas those in blue indicate the stiffest regions. LPA elicits the formation of actin stress fibers and transient global stiffening of the cytoskeleton. Bradykinin has little effect on the intracellular mechanical properties, whereas PDGF induces local stiffening of the cell periphery.

friction coefficient of the particle and their mean speed  $v$ ,  $F = f v$ . Here,  $f = 6\pi\eta a$  is the friction coefficient of the particle, which is assumed to be spherical;  $a$  is its radius;  $\eta$  is the mean shear viscosity of the intracellular region measured by ICM; and  $v$  is the previously reported mean velocity of the particles. For influenza viruses ( $v = 1\text{--}4 \mu\text{m/s}$ ;  $a = 80\text{--}120 \text{ nm}$ ) (Lakadamyali *et al.*, 2003), gene carriers ( $v = 0.2 \mu\text{m/s}$ ;  $a = 160 \text{ nm}$ ) (Suh *et al.*, 2003), and vesicles ( $v = 0.6 \mu\text{m/s}$ ;  $a = 200 \text{ nm}$ ) (Tvarusko *et al.*, 1999), the corresponding forces due to friction in migrating cells are  $\sim 7\text{--}42$ , 2.8, and 10.5 pN, respectively. These forces are larger than those generated by the motor proteins kinesin ( $\sim 5 \text{ pN}$ ) (Meyhofer and Howard, 1995) and dynein ( $\sim 1 \text{ pN}$ ) (Mallik *et al.*, 2004), suggesting that multiple motors must be working together to move these particles through the cell. Our measurements indicate that on average, the forces required for the net movement of  $0.1\text{-}\mu\text{m}$  vesicles along microtubules in migrating fibroblasts are almost 4 times larger than those required in quiescent fibroblasts. The required forces become significantly larger when vesicles are directed toward the leading edge of the cell.

Our ICM results obtained from nocodazole-treated cells suggests that the observed spatial orientation of the mechanical properties of Swiss 3T3 fibroblasts at the edge of a wounded monolayer is in part regulated by microtubules. Complete disassembly of microtubules resulted in inhibition of wound closure and loss of micromechanical polarity; however, the overall morphology of the cell remained unaffected. Interestingly, microtubule depolymerization did

not significantly affect the overall mechanical properties of the cell. These results suggest that microtubules act upstream of actin network formation and supports the hypothesis that microtubules contribute to cell motility through the stabilization of the leading edge via direct promotion of lamellipodia protrusion (Wittmann and Waterman-Storer, 2001).

## ACKNOWLEDGMENTS

This work has been supported by a National Aeronautics and Space Administration grant (NAG9-1563) and a National Science Foundation grant (CTS0210718) (to D.W. and Y.T.). T.P.K. was supported by a National Aeronautics and Space Administration training grant (NGT965).

## REFERENCES

- Berg, H. C. (1993). *Random Walks in Biology*, Princeton, NJ: Princeton University Press.
- Bershadsky, A. D., Vaisberg, E. A., and Vasiliev, J. M. (1991). Pseudopodial activity at the active edge of migrating fibroblast is decreased after drug-induced microtubule depolymerization. *Cell Motil. Cytoskeleton* *19*, 152–158.
- Borisy, G. G., and Svitkina, T. M. (2000). Actin machinery: pushing the envelope. *Cur. Opin. Cell Biol.* *12*, 104–112.
- Chandrasekhar, S. (1943). Stochastic problems in physics and astronomy. *Rev. Mod. Phys.* *15*, 1–89.
- Coulombe, P. A., Bousquet, O., Ma, L., Yamada, S., and Wirtz, D. (2000). The 'ins' and 'outs' of intermediate filament organization. *Trends Cell Biol.* *10*, 420–428.
- Cramer, L. P., Briggs, L. J., and Dawe, H. R. (2002). Use of fluorescently labeled deoxyribonuclease I to spatially measure G-actin levels in migrating and non-migrating cells. *Cell Motil. Cytoskeleton* *51*, 27–38.
- Crocker, J. C., Valentine, M. T., Weeks, E. R., Gislser, T., Kaplan, P. D., Yodh, A. G., and Weitz, D. A. (2000). Two-point microrheology of inhomogeneous soft materials. *Phys. Rev. Lett.* *85*, 888–891.
- Dasgupta, B. R., Tee, S. Y., Crocker, J. C., Frisken, B. J., and Weitz, D. A. (2002). Microrheology of polyethylene oxide using diffusing wave spectroscopy and single scattering. *Phys. Rev. E Stat. Nonlin. Soft. Matter Phys.* *65*, 051505.
- DeBiasio, R., Bright, G. R., Ernst, L. A., Waggoner, A. S., and Taylor, D. L. (1987). Five-parameter fluorescence imaging: wound healing of living Swiss 3T3 cells. *J. Cell Biol.* *105*, 1613–1622.
- Eckstein, A., Suhm, J., Friedrich, C., Maier, R. D., Sassmannshausen, J., Bochmann, M., and Mulhaupt, R. (1998). Determination of plateau moduli and entanglement molecular weights of isotactic, syndiotactic, and atactic polypropylenes synthesized with metallocene catalysts. *Macromolecules* *31*, 1335–1340.
- Einstein, A. (1905). Über die von der molekularkinetischen Theorie der Wärme geforderte Bewegung von in ruhenden Flüssigkeiten suspendierten Teilchen. *Ann. Physik* *17*, 549
- Flanagan, L. A., Chou, J., Falet, H., Neujahr, R., Hartwig, J. H., and Stossel, T. P. (2001). Filamin A, the Arp2/3 complex, and the morphology and function of cortical actin filaments in human melanoma cells. *J. Cell Biol.* *155*, 511–517.
- Goldman, R. D. (1971). The role of three cytoplasmic fibers in BHK-21 cell motility. I. Microtubules and the effects of colchicine. *J. Cell Biol.* *51*, 752–762.
- Gundersen, G. G. (2002). Evolutionary conservation of microtubule-capture mechanisms. *Nat. Rev. Mol. Cell. Biol.* *3*, 296–304.
- Haber, C., Alom-Ruiz, S., and Wirtz, D. (2000). Shape anisotropy of a single random-walk polymer. *Proc. Natl. Acad. Sci. USA* *97*, 10792–10795.
- Heidemann, S. R., and Wirtz, D. (2004). Towards a regional approach to cell mechanics. *Trends Cell Biol.* *14*, 160–166.
- Holzwarth, G., Bonin, K., and Hill, D. B. (2002). Forces required of kinesin during processive transport through cytoplasm. *Biophys. J.* *82*, 1784–1790.
- Janmey, P. A., Hvidt, S., Lamb, J., and Stossel, T. P. (1990). Resemblance of actin-binding protein/actin gels to covalently crosslinked networks. *Nature* *345*, 89–92.
- Kole, T. P., Tseng, Y., Huang, L., Katz, J. L., and Wirtz, D. (2004a). Rho kinase regulates the intracellular micromechanical response of adherent cells to Rho activation. *Mol. Biol. Cell* *15*, 3475–3484.

- Kole, T. P., Tseng, Y., and Wirtz, D. (2004b). Intracellular microrheology as a tool for the measurement of the local mechanical properties of live cells. *Methods Cell Biol.* 78.
- Kozma, R., Ahmed, S., Best, A., and Lim, L. (1995). The Ras-related protein Cdc42Hs and bradykinin promote formation of peripheral actin microspikes and filopodia in Swiss 3T3 fibroblasts. *Mol. Cell Biol.* 15, 1942–1952.
- Kraynov, V. S., Chamberlain, C., Bokoch, G. M., Schwartz, M. A., Slabaugh, S., and Hahn, K. M. (2000). Localized Rac activation dynamics visualized in living cells. *Science* 290, 333–337.
- Lakadamyali, M., Rust, M. J., Babcock, H. P., and Zhuang, X. (2003). Visualizing infection of individual influenza viruses. *Proc. Natl. Acad. Sci. USA* 100, 9280–9285.
- Lauffenburger, D. A., and Horwitz, A. F. (1996). Cell migration: a physically integrated molecular process. *Cell* 84, 359–369.
- Magdalena, J., Millard, T. H., and Machesky, L. M. (2003). Microtubule involvement in NIH 3T3 Golgi and MTOC polarity establishment. *J. Cell Sci.* 116, 743–756.
- Mallik, R., Carter, B. C., Lex, S. A., King, S. J., and Gross, S. P. (2004). Cytoplasmic dynein functions as a gear in response to load. *Nature* 427, 649–652.
- Maniotis, A. J., Chen, C. S., and Ingber, D. E. (1997). Demonstration of mechanical connections between integrins, cytoskeletal filaments, and nucleoplasm that stabilize nuclear structure. *Proc. Natl. Acad. Sci. USA* 94, 849–854.
- Mason, T. G., Ganesan, K., van Zanten, J. V., Wirtz, D., and Kuo, S. C. (1997). Particle-tracking microrheology of complex fluids. *Phys. Rev. Lett.* 79, 3282–3285.
- Mason, T. G., and Weitz, D. (1995). Optical measurements of frequency-dependent linear viscoelastic moduli of complex fluids. *Phys. Rev. Lett.* 74, 1254–1256.
- Meyhofer, E., and Howard, J. (1995). The force generated by a single kinesin molecule against an elastic load. *Proc. Natl. Acad. Sci. USA* 92, 574–578.
- Mitchison, T. J., and Cramer, L. P. (1996). Actin-based cell motility and cell locomotion. *Cell* 84, 371–379.
- Mogilner, A., and Oster, G. (1996). Cell motility driven by actin polymerization. *Biophys. J.* 71, 3030–3045.
- Mogilner, A., and Oster, G. (2003). Force generation by actin polymerization II: the elastic ratchet and tethered filaments. *Biophys. J.* 84, 1591–1605.
- Nagayama, M., Haga, H., and Kawabata, K. (2001). Drastic change of local stiffness distribution correlating to cell migration in living fibroblasts. *Cell Motil. Cytoskeleton* 50, 173–179.
- Nobes, C. D., and Hall, A. (1999). Rho GTPases control polarity, protrusion, and adhesion during cell movement. *J. Cell Biol.* 144, 1235–1244.
- Peskin, C. S., Odell, G. M., and Oster, G. F. (1993). Cellular motions and thermal fluctuations: the Brownian ratchet. *Biophys. J.* 65, 316–324.
- Pollard, T. D. (2003). The cytoskeleton, cellular motility and the reductionist agenda. *Nature* 422, 741–745.
- Pollard, T. D., and Borisy, G. G. (2003). Cellular motility driven by assembly and disassembly of actin filaments. *Cell* 112, 453–465.
- Qian, H., Sheetz, M. P., and Elson, E. L. (1991). Single particle tracking. Analysis of diffusion and flow in two-dimensional systems. *Biophys. J.* 60, 910–921.
- Ridley, A. J., Paterson, H. F., Johnston, C. L., Diekmann, D., and Hall, A. (1992). The small GTP-binding protein Rac regulates growth-factor induced membrane ruffling. *Cell* 70, 401–410.
- Ridley, A. J., Schwartz, M. A., Burridge, K., Firtel, R. A., Ginsberg, M. H., Borisy, G., Parsons, J. T., and Horwitz, A. R. (2003). Cell migration: integrating signals from front to back. *Science* 302, 1704–1709.
- Rodriguez, O. C., Schaefer, A. W., Mandato, C. A., Forscher, P., Bement, W. M., and Waterman-Storer, C. M. (2003). Conserved microtubule-actin interactions in cell movement and morphogenesis. *Nat. Cell Biol.* 5, 599–609.
- Sato, M., Schwarz, W. H., and Pollard, T. D. (1987). Dependence of the mechanical properties of actin/ $\alpha$ -actinin gels on deformation rate. *Nature* 325, 828–830.
- Sheetz, M. P., Wayne, D. B., and Pearlman, A. L. (1992). Extension of filopodia by motor-dependent actin assembly. *Cell Motil. Cytoskeleton* 22, 160–169.
- Stossel, T. P. (1993). On the crawling of animal cells. *Science* 260, 1086–1094.
- Suh, J., Wirtz, D., and Hanes, J. (2003). Efficient active transport of gene nanocarriers to the cell nucleus. *Proc. Natl. Acad. Sci. USA* 100, 3878–3882.
- Tseng, Y., An, K. M., Esue, O., and Wirtz, D. (2004). The bimodal role of filamin in controlling the architecture and mechanics of F-actin networks. *J. Biol. Chem.* 279, 1819–1826.
- Tseng, Y., Kole, T. P., Lee, S.H.J., and Wirtz, D. (2002a). Local dynamics and viscoelastic properties of cell biological systems. *Curr. Opin. Colloid Interface Sci.* 7, 210–217.
- Tseng, Y., Kole, T. P., and Wirtz, D. (2002b). Micromechanical mapping of live cells by multiple-particle-tracking microrheology. *Biophys. J.* 83, 3162–3176.
- Tseng, Y., and Wirtz, D. (2001). Mechanics and multiple-particle tracking microheterogeneity of alpha-actinin-cross-linked actin filament networks. *Biophys. J.* 81, 1643–1656.
- Tvarusko, W., Bentele, M., Misteli, T., Rudolf, R., Kaether, C., Spector, D. L., Gerdes, H. H., and Eils, R. (1999). Time-resolved analysis and visualization of dynamic processes in living cells. *Proc. Natl. Acad. Sci. USA* 96, 7950–7955.
- Vasiliev, J. M., Gelfand, I. M., Domnina, L. V., Ivanova, O. Y., Komm, S. G., and Olshevskaja, L. V. (1970). Effect of colcemid on the locomotory behaviour of fibroblasts. *J. Embryol. Exp. Morphol.* 24, 625–640.
- Wachsstock, D., Schwarz, W. H., and Pollard, T. D. (1994). Crosslinker dynamics determine the mechanical properties of actin gels. *Biophys. J.* 66, 801–809.
- Wittmann, T., and Waterman-Storer, C. M. (2001). Cell motility: can Rho GTPases and microtubules point the way? *J. Cell Sci.* 114, 3795–3803.
- Xu, J., Tseng, Y., and Wirtz, D. (2000). Strain-hardening of actin filament networks - regulation by the dynamic crosslinking protein  $\alpha$ -actinin. *J. Biol. Chem.* 275, 35886–35892.
- Xu, J., Viasnoff, V., and Wirtz, D. (1998). Compliance of actin filament networks measured by particle-tracking microrheology and diffusing wave spectroscopy. *Rheologica Acta* 37, 387–398.